
Proceedings Paper:
Allanic, R., Le Berre, D., Quendo, C. et al. (5 more authors) (2023) Silicon carbide antenna for polarization agility in constrained environments. In: 2023 IEEE Conference on Antenna Measurements and Applications (CAMA). 2023 IEEE Conference on Antenna Measurements and Applications (CAMA), 15-17 Nov 2023, Genoa, Italy. Institute of Electrical and Electronics Engineers (IEEE) , pp. 653-656. ISBN 9798350323054

https://doi.org/10.1109/cama57522.2023.10352662

Silicon Carbide Antenna for Polarization Agility in Constrained Environments

Rozenn Allanic[1], Denis Le Berre[1], Cédric Quendo[1]
Univ. Brest, Lab-STICC
CNRS, UMR 6285
Brest, France
Rozenn.Allanic@univ-brest.fr

Edward A Ball[2], Jo Shien Ng[2], Guanwei Huang[2]
The University of Sheffield, Dept of Electronic & Electrical Engineering
Sheffield, UK
j.s.ng@sheffield.ac.uk

Aude Leuliet[3], Thomas Merlet[3]
Thales LAS OME
Élancourt, France
thomas.merlet@thalesgroup.com

***Abstract*— This paper highlights the advantages of designing a reconfigurable antenna on silicon carbide (SiC) substrate. The semiconductor properties of the SiC allows co-design of the antenna and the active elements. Co-design meets the objectives of stability at high temperatures, high-power management, high-performance, a high level of integration and cost-effectiveness. The proposed patch antenna works at 12.1 GHz switching from a linear polarization to a circular one. Reconfigurability is achieved using a distributed doped area, forming a serial integrated junction in the substrate.**

Keywords*— *Antenna, polarization, reconfigurable, silicon carbide (SiC), ScDDAs, tunable.

I. Introduction

Microwave antennas are one of the key elements present in all communicating systems. Antenna polarization needs to be compatible between transmitters and receivers to optimize the communication quality. To avoid the misalignment problems between two antennas, one solution is to physically relocate the complete system, or alternatively, to design polarization reconfigurable antennas. In the literature, polarization reconfigurability is mainly achieved using liquid metal [1] or dielectric liquid [2] or PIN diodes [3]-[5]. These solutions suffer from manufacture complexities or parasitic effects with the surface-mounted components inducing impedance mismatching and additional losses. A novel solution uses semi-conductor distributed doped areas [6], which enables co-designing the antenna and the active elements, with reduced steps in the whole process. This permits an optimization of the overall function and offers better integration and with a commutation with a low bias voltage. Here, the idea is to design a reconfigurable antenna taking the advantage of a co-design method such as in [7] on a silicon carbide (SiC) substrate [8]. Indeed, SiC substrate is a good candidate for high constraints environments for their temperature and power stability performances.

This way, Section II presents the antenna design for polarization agility. Section III deals with the electromagnetic simulations, before in Section IV details the manufacture steps followed in Section V by the measurement setup and the results. Finally, the conclusion is proposed in Section VI.

II. Antenna Design

Figure 1 shows the design of the reconfigurable antenna. This antenna consists of a square patch with two truncated corners, one of which can be connected to a triangle using an active element. The antenna is designed on a 4H-SiC substrate, which allows the co-design of the antenna and doped areas to make the antenna agile. The active element is an integrated serial junction (in red in Fig. 1) with two highly doped areas (P^+ and N^+) whose position, size and shape can be chosen to optimize the antenna's performance.

Biasing the junction either isolates or connects the corner to the antenna. Figure 2 (a) shows a side view of the antenna to give an illustration of the integrated junction. Figures 2 (b) and (c) present some simplified models of the integrated junction in the two working states. In the OFF-state, the junction is considered without being biased, the switch is opened. In the ON-state, the junction is in forward bias, the switch is closed. Therefore, without DC biasing the junction, the antenna has two truncated corners and operates in linear polarization (LP). When the junction is forward biased, the antenna has only one truncated corner and operates in circular polarization (CP).

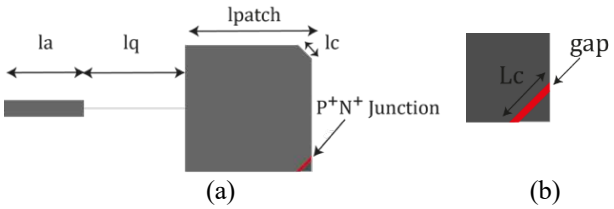

Fig. 1. (a) Layout of the reconfigurable antenna. (b) Zoom on the integrated junction.

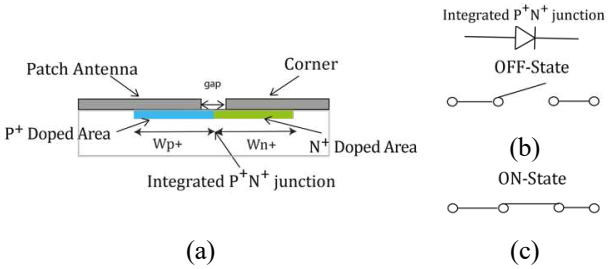

Fig. 2. (a) Side view, Zoom on the integrated junction. (b) Simplified model of the reverse bias integrated junction. (c) Simplified model of the forward bias integrated junction.

III. Simulated Results

To validate the idea, Table 1 gives the antenna dimension. This was designed on a 350-µm semi-isolating substrate, without taking into account dielectric losses. The antenna behavior was simulated using the ANSYS® HFSS™ software. The dielectric permittivity of the substrate is fixed at 10.3. The junction is first approximated as an ideal switch, removed in LP (OFF-state). In CP (ON-state), the junction is simulated as an aluminum contact. Figure 3 shows the reflection coefficient in both-states, the antenna resonates at 12.28 GHz in the OFF-state and 12.16 GHz in the ON-state. The reflection coefficient is lower than -10 dB around 12.25 GHz in both states. Figures 4 (a) and (b) illustrate the electrical field for two different phases at the input port in LP and in CP. Therefore, in the OFF-state, the electrical field is the same whatever the phase at the input port, whereas in the ON-state, the electrical field rotates depending on the phase at the input port. Table 2 presents the simulated antenna performances in both-states. In the OFF-state, the realized

gain is higher than 4.5 dB in a linear polarization with an axial ratio higher than 40 dB, due to the linear polarization. Then, in the ON-state, the realized gain is of 5.5 dB with an axial ratio of 1.8 dB, this confirms the circular polarization. Figure 5 shows the final antenna design. Indeed, a transition from coplanar waveguide to microstrip was added to avoid using a SMA connector. Moreover, a bias circuit was also added in order to apply a DC voltage between the two parts of the integrated junction. The dimensions of these additional parts are summed up in Table 3.

Table 1. Dimensions in mm of the patch antenna.

la	wa	lq	Wq	lpatch	lc	gap	Wp+	Wn+
1.5	0.5	3	0.01	3.75	2.2	0.04	0.13	0.13

Wx stand for each respected length.

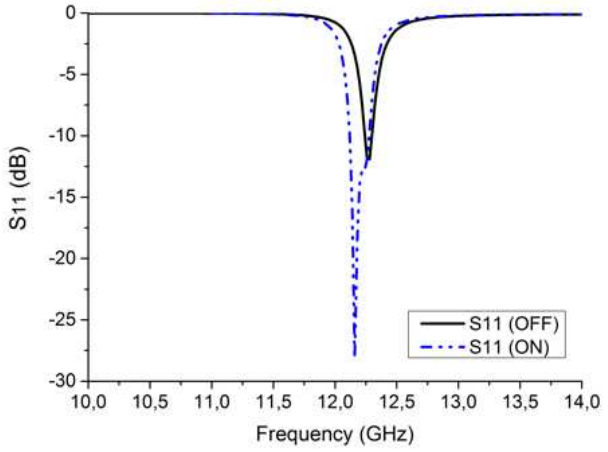

Fig. 3. EM Simulated results of the reflection coefficient in both states.

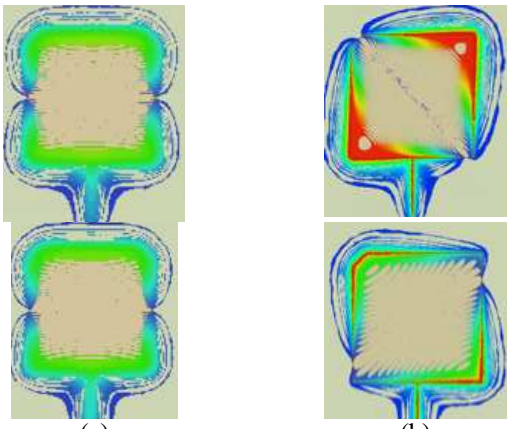

(a) (b)

Fig. 4. (a) Electrical field with two different phases in LP. (b) Electrical field with two different phases in CP.

Table 2. Antenna performances in both-states.

	OFF-state	ON-state
Frequency (GHz)	12.28	12.16
S11 (dB)	-12	-28
Realized Gain (dB)	4.5	5.5
Polarization	Linear	Circular
AR (dB)	> 40	1.8

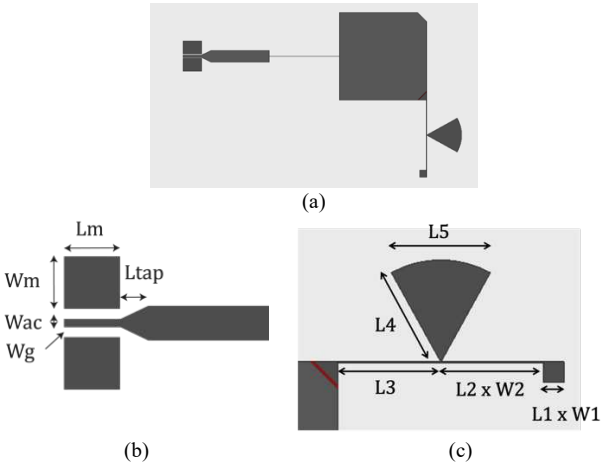

Fig. 5. (a) Final antenna design before manufacture. (b) zoom on the coplanar to microstrip transition. (c) Zoom on the bias circuit polarization.

Table 3. Dimensions in mm of coplanar access and the bias circuit

Wm	Lm	Ltap	Wac	Wg		
0.55	0.8	0.39	0.114	0.044		
L1	W1	L2	W2	L3	L4	L5
0.3	0.3	1.5	0.024	1.5	1.49	1.45

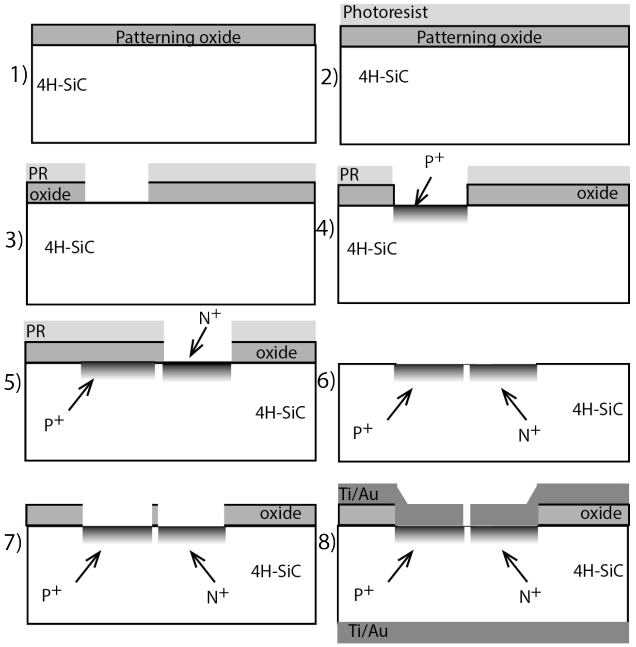

Fig. 6. Manufacturing process steps.

IV. Fabrication

The manufacture was done on a 350-µm thick 4H-SiC semi-insulating substrate. The process steps are summed up in Fig. 6. Five masks are required for alignment marks, implantation of p (Boron) and n (Nitrogen), dielectric opening and top metal contact.

The fabrication process started with creating an alignment mark which then were dry etched into the substrate. Since relatively high implant energy was chosen, a 1-µm SiO2 was deposited as pattering oxide to protect the undoped area instead of normal photoresist for both p and n implantation.

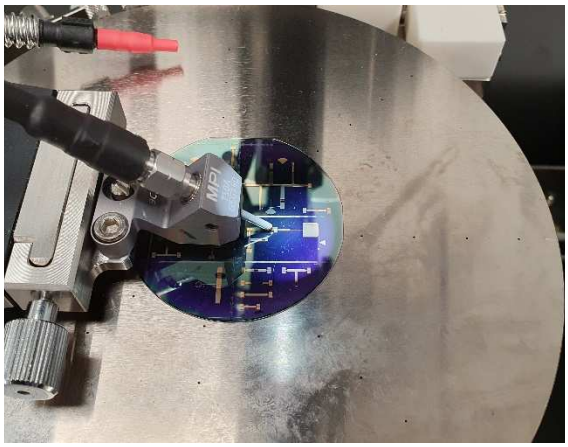

Fig. 7. Fabricated antenna on main prober at [9].

After patterning the doped area, the patterning oxide was dry etched to the substrate followed by a 30 nm screening oxide deposition. Both implanted target depth for p and n is 500 nm with doping concentration higher than 1E+18 cm^{-3}. It was observed that the color of the implanted area became dark due to the crystal damage from implantation, and then it was removed by rapid thermal annealing at a very high temperature (>1400°C). A 600 nm fresh oxide was deposited and then the doped area was opened by standard photolithography with the dielectric opening mask. Finally, metal Ti/Au with a thickness of 40/400 nm was deposited on the top and bottom of the substrate without further annealing.

V. Measured Results

Figure 7 shows the fabricated antenna on the main probe station and Fig. 8 illustrates the antenna undergoing radiated test on special mini prober station (phi sweep is vertically downwards). Tests were jointly performed at The University of Brest and at The UKRI National mmWave Measurement Laboratory [9] at the University of Sheffield. Unfortunately, the process steps were not able to achieve quantity of doping atoms as high as required. This implies that the integrated junction is not working in the ON-state, and the measured results are only presented in their OFF-state.

A comparison of the reflection coefficient simulated and measured results is given in Fig. 9. There is a slight shift in the resonant frequency measured at 12.1 GHz instead of 12.25 GHz. This is probably due to a slight difference on the dielectric permittivity between the one used in the simulation and the real one. The wafer probes affect the radiated gain measurements for certain cuts, so Fig. 10 shows the results of phi cut at theta position of maximum gain. The maximum gain measured was 0 dBi.

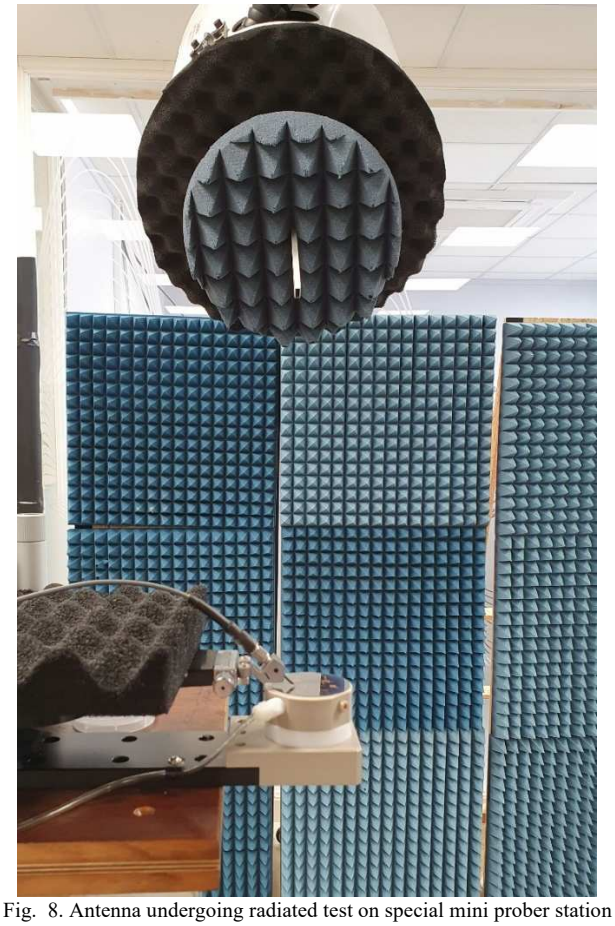

Fig. 8. Antenna undergoing radiated test on special mini prober station (phi sweep is vertically downwards as viewed here) [9].

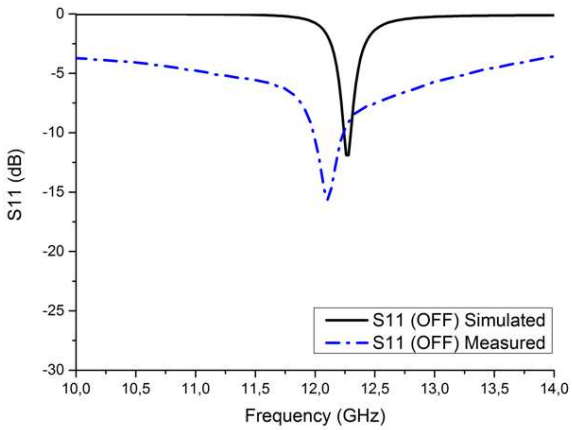

Fig. 9. Comparison between simulated and measured results of the reflection coefficient in the OFF-state.

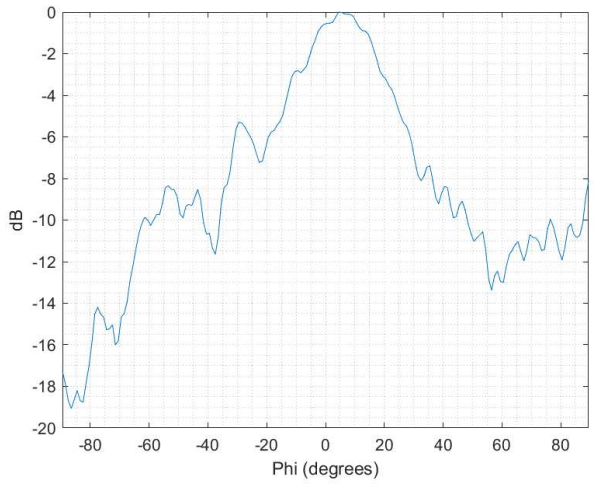

Fig. 10. Normalized Measured Radiation Pattern at location of peak power (diodes unbiased).

VI. Conclusion

In this paper, a monolithic reconfigurable antenna for polarization agility was presented. Despite the integrated junction is not working, the antenna performances in the OFF-state are promising. The monolithic manufacture of both parts could be an answer to a frequency rise. Using a 4H-SiC substrate, the antenna could work in constraints environment.

Acknowledgment

The authors would like to thank both governmental agencies in UK and France, namely DSTL and DGA, for their financial support operated in the frame of the MCM ITP (Material & Components for Missiles, Innovation Technology Partnership). The authors also would like to thank the TECHYP platform (the High Performance Computing Cluster at Lab-STICC) thanks to which the devices could be simulated. The authors would like to thank Steve Marsden, Dr. Sumin David Joseph and Sideqe Askre for wafer testing at the EPSRC National mmWave Measurement Lab.

References

[1] X. Yan *et al*., "Polarization Reconfigurable Filtering Patch Antenna Using Liquid Metal," *IEEE International Workshop on Electromagnetics: Applications and Student Innovation Competition (iWEM)*, Guangzhou, China, 2021.

[2] J. Ren *et al*., "Radiation Pattern and Polarization Reconfigurable Antenna Using Dielectric Liquid," in *IEEE Transactions on Antennas and Propagation*, vol. 68, no. 12, pp. 8174-8179, Dec. 2020, doi: 10.1109/TAP.2020.2996811.

[3] P. Pan and B. Guan, "A Wideband Polarization Reconfigurable Antenna with Six Polarization States," *2018 12th International Symposium on Antennas, Propagation and EM Theory (ISAPE)*, Hangzhou, China, 2018, pp. 1-4, doi: 10.1109/ISAPE.2018.8634224.

[4] T. Song *et al*., "A polarization reconfigurable microstrip patch antenna using PIN diodes," *IEEE Asia Pacific Microwave Conference Proceedings*, Kaohsiung, Taiwan, 2012.

[5] W. Li, Y. M. Wang, Y. Hei, B. Li and X. Shi, "A Compact Low-Profile Reconfigurable Metasurface Antenna With Polarization and Pattern Diversities," in *IEEE Antennas and Wireless Propagation Letters*, vol. 20, no. 7, pp. 1170-1174, July 2021, doi: 10.1109/LAWP.2021.3074639.

[6] R. Allanic *et al*., "On-Chip Polarization Reconfigurable Microstrip Patch Antennas Using Semiconductor Distributed Doped Areas (ScDDAs)". *Electronics* 2022, *11*, 1905.

[7] R. Allanic *et al*., "Three-State Microwave Tunable Resonator Integrating Several Active Elements on Silicon Technology in a Global Design," in *IEEE Microwave and Wireless Components Letters*, vol. 28, no. 2, pp. 141-143, 2018.

[8] T. Karacolak, *et al.,* "Silicon Carbide (SiC) Antennas for High-Temperature and High-Power Applications," in *IEEE Antennas and Wireless Propagation Letters*, vol. 12, 2013.

[9] The National mmWave Measurement Laboratory. [Online]. Available: https://mmwave.group.shef.ac.uk/.